2019 IEEE 58th Conference on Decision and Control (CDC)
Palais des Congrès et des Expositions Nice Acropolis
Nice, France, December 11-13, 2019

Frequency Regulation using Sparse Learned Controllers in Power Grids with Variable Inertia due to Renewable Energy

Patricia Hidalgo-Gonzalez, Rodrigo Henriquez-Auba, Duncan S. Callaway and Claire J. Tomlin

Abstract— **Inertia from rotating masses of generators in power systems influence the instantaneous frequency change when an imbalance between electrical and mechanical power occurs. Renewable energy sources (RES), such as solar and wind power, are connected to the grid via electronic converters. RES connected through converters affect the system's inertia by decreasing it and making it time-varying. This new setting challenges the ability of current control schemes to maintain frequency stability. Proposing adequate controllers for this new paradigm is key for the performance and stability of future power grids. The contribution of this paper is a framework to learn sparse time-invariant frequency controllers in a power system network with a time-varying evolution of rotational inertia. We model power dynamics using a Switched-Affine hybrid system to consider different modes corresponding to different inertia coefficients. We design a controller that uses as features, i.e. input, the systems states. In other words, we design a control proportional to the angles and frequencies. We include virtual inertia in the controllers to ensure stability. One of our findings is that it is possible to restrict communication between the nodes by reducing the number of features in the controller (from 22 to 10 in our case study) without disrupting performance and stability. Furthermore, once communication between nodes has reached a threshold, increasing it beyond this threshold does not improve performance or stability. We find a correlation between optimal feature selection in sparse controllers and the topology of the network.**

I. INTRODUCTION

As renewable energy resources (RES) continue to increase their participation in power systems [1], [2], different challenges arise. For example, solar and wind power show variability and uncertainty in their electricity generation [3], making optimal power flow a more complex task for system operators. In the case of power system dynamics, voltage and frequency control can become an issue due to high penetration of solar power [4] and increasing participation of inverter connected RES [5] respectively.

Frequency deviation from its nominal value occurs when there is an instantaneous mismatch between electricity generation and demand. The first response to this frequency excursion comes from the inertia of the power system. This inertial response originates from the kinetic energy supplied to the grid by the synchronous generators currently connected to it. Droop or governor response is the second mechanism that addresses frequency deviations [6]. Droop control is an automatic control proportional to the deviation in frequency. Slower mechanisms (e.g. spinning reserves) also participate to restore frequency to its nominal value [6].

RES connected to the grid, such as solar and wind power, use inverters. In general, inverters do not provide any inertia to the power system, which results in a lower and time-varying system-wide inertia. Therefore, a grid with increasing penetration of RES will result in a less effective inertial response to frequency deviations. This increases the variation of frequency under abrupt imbalances in generation and demand. The aforementioned can lead to cases in which classical frequency control schemes are not fast enough to contain contingencies [7].

A solution that has been studied for systems with low inertia is to use inverters and storage to provide inertia. This is generally referred to as virtual inertia: a controller proportional to the derivative of the frequency. Previous work studying virtual inertia can be found in the literature [8]–[14]. Our previous publication [15], proposes for the first time a new modeling framework for power system dynamics to simulate a time-varying evolution of inertia in the network due to the time dependent participation of RES. We model power dynamics using a Switched-Affine hybrid system to consider different modes corresponding to different inertia coefficients. Time-varying power system dynamics pose a new set of challenges for frequency control. Now control design must take into account the time dependence of the dynamical model.

In recent years, techniques from machine learning have become popular in the field of control design [16], [17]. Interesting applications have been developed for distributed control of power flow in power systems [18], [19]. In [20] we design a fixed and stable frequency controller under the paradigm of time-varying inertia. We use angles, frequencies and derivatives of the frequencies as features or input for the controllers. An interesting question that stems from this work is the potential trade-off of restricting communication between controllers. Information availability between nodes entails a cost (sensing and broadcasting), thus designing communication restricted control schemes, i.e. sparse controllers, is of particular interest in power systems. In a similar line of thought, [21] studies from an information theoretic approach, the trade-off between performance and communication between control agents.

In this paper we study how sparsity can be induced in a time-invariant learned controller for a time-varying dynamical system. This application is of particular interest because

Patricia Hidalgo-Gonzalez and Duncan S. Callaway are with the Department of Electrical Engineering and Computer Sciences and the Energy and Resources Group, University of California, Berkeley, CA 94720, USA. [patricia.hidalgo.g, dcal]@berkeley.edu

Rodrigo Henriquez-Auba, and Claire J. Tomlin are with the Department of Electrical Engineering and Computer Sciences, University of California, Berkeley, CA 94720, USA. [rhenriquez, tomlin]@berkeley.edu

978-1-7281-1398-2/19/$31.00 ©2019 IEEE

of its potential for aiding safe RES integration. Additionally, power system dynamics are a relevant application for this control research question thanks to the added complexity of operating on a graph (transmission network). Finally, information availability between nodes entails a cost (sensing and broadcasting), thus designing communication-restricted control schemes is of particular interest in power systems.

The contribution of this paper is the design of a sparse and guaranteed stable time-invariant frequency controller for time-varying power dynamics. We also test the improvement in performance metrics and stability of introducing more features to the controller than the minimum identified. Our work can be summarized as follows:

- In the time-varying framework for power dynamics, we design a controller with fixed gains, proportional to the system's states (angles and frequencies). We design the controller by learning its parameters from a training set generated by optimally solving a Model Predictive Control (MPC) problem for different scenarios of frequency regulation. We add virtual inertia to the controller to guarantee stability in all inertia modes [20].
- To test how sparse our learned controller can be and to investigate the trade-off between communication requirements and performance/stability we use a Lasso regression [22] for the controller at each node. We vary widely the sensitivity parameter associated to the regularization term in the learning problem.
- We shed light on the relevance of graph topology and optimal feature selection for the learned controller at each node.
- We show for some cases that it is not possible for the learned controller to steer frequency deviation back to zero when facing inertia coefficients that are not included in the training set. This validates the importance of controller design taking into account time-varying power dynamics.

We conclude that it is possible to design via learning a sparse, time-invariant and stable controller for the hybrid power dynamics formulation. Furthermore, we show that it is possible to reduce the number of features in the controller (from 22 to 10 in our case study) without disrupting performance and stability. Additionally, we depict how enabling more communication beyond a threshold does not improve performance or stability.

The rest of the paper is organized as follows: Section II presents the problem formulation, Section III covers simulations, performance and stability analyses, and Section IV concludes with our main findings and future work.

II. PROBLEM FORMULATION

A. Power system dynamics as a hybrid system

We model an electric power system network as a graph with n nodes and $n(n-1)/2$ possible edges. Using the direct current approximation for power flow, we can write the swing equation [14] as

$$m_i\ddot{\theta}_i + d_i\dot{\theta}_i = p_i - \sum_{j\in\mathcal{N}_i} b_{ij}(\theta_i-\theta_j), \quad i\in\{1,\dots,N\} \tag{1}$$

where m_i corresponds to the equivalent rotational inertia in node i, d_i is the droop control or frequency damping coefficient, p_i represents net power injection at node i, $\mathcal{N}_i$ is set of nodes connected by an edge to node i, b_{ij} is the susceptance of the transmission line between nodes i and j, and θ_i is the voltage phase angle at node i. The state space representation of the model can be written as

$$\begin{bmatrix}\dot{\theta}\\ \dot{\omega}\end{bmatrix} = \begin{bmatrix}0 & I\\ -M^{-1}L & -M^{-1}D\end{bmatrix}\begin{bmatrix}\theta\\ \omega\end{bmatrix} + \begin{bmatrix}0\\ M^{-1}\end{bmatrix} p_{\text{in}} \tag{2}$$

where the states correspond to the stacked vector of angles and frequencies at each node $(\theta^\top,\omega^\top)^\top\in\mathbb{R}^{2n}$, the frequency, ω, is the derivative of the angle, i.e. $\omega=\dot{\theta}$, $M=\text{diag}(m_i)$ is a diagonal matrix with rotational inertia coefficients, $D=\text{diag}(d_i)$ is a diagonal matrix with droop control coefficients, I is the $n\times n$ identity matrix, p_{in} corresponds to the power input, and $L\in\mathbb{R}^{n\times n}$ is the Laplacian of the network. The network Laplacian is defined as $\ell_{ij}=-b_{ij}$ when $i\neq j$, and $\ell_{ii}=\sum_{j\in\mathcal{N}_i} b_{ij}$.

Traditionally, the equivalent rotational inertia of a power system has been modeled as a constant over time due to the predominance of thermal generators. Nonetheless, the increasing penetration of RES has lowered and transformed its nature into a time-varying coefficient [7], [23]. This study uses the modeling framework first introduced in [15] to represent the time dependence in inertia at each node. Frequency dynamics are modeled as a Switched-Affine hybrid system, where each mode has a predetermined set of values of equivalent inertia m_i at each node. The evolution of the inertia on the system depends on the current online generators and the connected power electronics converters. In this paper, the inertia at each time step t evolves as an exogenous input. Thus, power dynamics are given by

$$\begin{bmatrix}\dot{\theta}\\ \dot{\omega}\end{bmatrix} = \underbrace{\begin{bmatrix}0 & I\\ -M_{q(t)}^{-1}L & -M_{q(t)}^{-1}D\end{bmatrix}}_{\hat{A}_{q(t)}}\begin{bmatrix}\theta\\ \omega\end{bmatrix} + \underbrace{\begin{bmatrix}0\\ M_{q(t)}^{-1}\end{bmatrix}}_{\hat{B}_{q(t)}} p_{\text{in}} \tag{3}$$

where $M_{q(t)}$ represents the inertia matrix in the mode $q(t)\in\{1,\dots,m\}$. Using a zero-order hold discretization with time step T_s, we obtain the discretized time-varying dynamics

$$x_{t+1} = A_{q(t)}x_t + B_{q(t)}u_t \tag{4}$$

where x_t is the stacked vector of discretized angles and frequencies, $(\theta_t^\top,\omega_t^\top)^\top$, u_t is the discretized control action by generators and converters, $A_{q(t)}=\exp(\hat{A}_{q(t)}T_s)$ and $B_{q(t)}=\int_0^{T_s}\exp(\hat{A}_{q(t)}\tau)\hat{B}_{q(t)}d\tau$.

B. Generation of training set from optimal frequency control

In order to learn a time-invariant controller, we generate a training set from solving an MPC formulation. We minimize an objective function where the states and controllers are decision variables

$$\begin{aligned}\min_{x,u}\ & \sum_{t=0}^{T} x_t^\top Q x_t + u_t^\top R u_t\\ \text{s.t.}\ & x_0 = x^{(0)}\\ & x_{t+1} = A_{q(t)}x_t + B_{q(t)}u_t,\ t\in\{0,T-1\}\end{aligned} \tag{5}$$

$Q \in \mathbb{R}^{2n\times 2n}$ is a positive semidefinite matrix, $R \in \mathbb{R}^{n\times n}$ is a positive definite matrix, $x^{(0)}$ is the initial state, and T is the time horizon. Depending on the modeling goal, matrices Q and R can be modified to promote a specific behavior. This is a Quadratic Programming problem that can be solved directly, using for example CVX [24]. We describe the specifications for the simulations of this work in III-A.

C. Learned controller enhancing sparsity

In the setting of hybrid power dynamics with variable inertia, our control design via learning has two objectives:

- Learn a time-invariant frequency controller of the form $u_t = K_{\mathrm{L}} x_t$, where K_{L} is a constant matrix.
- Explore to what extent communication between nodes can be restricted to design a stable frequency controller. Communication between nodes i and j has to occur when the (i,j) entry of K_{L} is nonzero.

To accomplish these objectives we use a Lasso regression [22], [25] to learn optimal controllers at each node. The training set $(x^{(s)}, u^{(s)})$ we utilize comes from the optimal solution to (5) under different initial states. Each trajectory or optimal solution $(x^{(s)}, u^{(s)})$ for a given initial state defines a scenario s, with $s = \{1,\dots,S\}$. We solve a Lasso regression for each node i as an independent controller $u_{i,t} = \beta_i^\top x_t$, where $\beta_i^\top \in \mathbb{R}^{1\times 2n}$ is a row vector that has as components the gains of the controller at node i (i.e. $K_{\mathrm{L}} = \left[\beta_1 \dots \beta_n\right]^\top$):

$$\min_{\beta_i} \sum_{s=1}^{S}\sum_{t=1}^{T} \left|\left| u_{i,t}^{(s)} - \beta_i^\top x_t^{(s)} \right|\right|_2^2 + \lambda ||\beta_i||_1 \qquad (6)$$

The states that multiply the resulting nonzero components of the vector $\beta_i^\top$ correspond to the features that node i uses for its controller $u_{i,t}$. We solve (6) for each node for a range of the regularization sensitivity parameter λ using cross-validation. We vary the sensitivity parameter λ from zero (Least-Squares, i.e. using all possible $2n$ states as features) up to a value that would result in only one nonzero coefficient in the vector β_i.

D. Incorporating virtual inertia in the control

As we show in [20], to guarantee stability of a learned controller for hybrid power dynamics with variable inertia we include virtual inertia: a controller proportional to the derivative of the frequency, $K_{\mathrm{V}}\dot{\omega}$. To provide some intuition, consider a fixed inertia continuous time system and assume a controller of the form

$$u = K_{\mathrm{L}}(\theta^\top, \omega^\top)^\top + K_{\mathrm{V}}\dot{\omega} = K_{\mathrm{L}}x + \tilde{K}_{\mathrm{V}}\dot{x} \qquad (7)$$

where $\tilde{K}_{\mathrm{V}} = [0 \;\; K_{\mathrm{V}}]$, then:

$$\dot{x} = \begin{bmatrix} 0 & I \\ -M^{-1}L & -M^{-1}D \end{bmatrix} x + \begin{bmatrix} 0 \\ M^{-1} \end{bmatrix} (K_{\mathrm{L}}x + \tilde{K}_{\mathrm{V}}\dot{x}) \qquad (8)$$

Rearranging terms the system can be written as

$$\begin{aligned} \dot{x} &= (I - \hat{B}_{q(t)}\tilde{K}_V)^{-1}(\hat{A}_{q(t)} + \hat{B}_{q(t)}K_{\mathrm{L}})x \\ &= \begin{bmatrix} I & 0 \\ 0 & I - M_{q(t)}^{-1}K_{\mathrm{V}} \end{bmatrix}^{-1} \\ &\quad \times \begin{bmatrix} 0 & I \\ -M_{q(t)}^{-1}(L - K_{\mathrm{L},\theta}) & -M_{q(t)}^{-1}(D - K_{\mathrm{L},\omega}) \end{bmatrix} x \\ &= \begin{bmatrix} 0 & I \\ -\tilde{M}_{q(t)}^{-1}(L - K_{\mathrm{L},\theta}) & -\tilde{M}_{q(t)}^{-1}(D - K_{\mathrm{L},\omega}) \end{bmatrix} x \end{aligned}$$

where $\tilde{M}_{q(t)} = M_{q(t)}(I - M_{q(t)}^{-1}K_{\mathrm{V}}) = M_{q(t)} - K_{\mathrm{V}}$ provides a new system wide equivalent inertia due to the virtual inertia controller K_{V}. To determine a proper K_{V} we utilize a heuristic using a bisection method. We assume K_{V} of the form $K_{\mathrm{V}} = k_{\mathrm{v}} I_{n\times n}$. We iterate over k_{v} until the closed loop system for each inertia mode has all its eigenvalues with negative real part, stabilizing the system's dynamics.

TABLE I

PARAMETERS FOR THE TWELVE-BUS THREE-REGION CASE STUDY [13], [15] AND [26].

Parameter	Value
Transformer reactance	0.15 p.u.
Line impedance	(0.0001 + 0.001j) p.u./km
Base voltage	230 kV
Base power	100 MVA
Droop control	1.5 %/%

III. SIMULATIONS AND ANALYSIS

A. Data and simulation description

We use MATLAB® to model a twelve-bus three-region network that has also been used in [13], [14], [15], and [20] and [26]. Each node has two states (angle and frequency). Table I shows the parameters of the network. Notice bus 11 is directly connected to 12, thus we are effectively simulating an $n = 11$ node network.

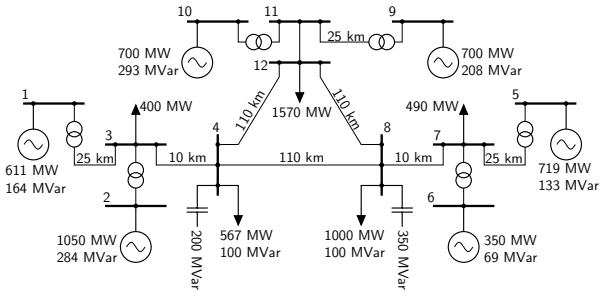

Fig. 1. Case study: Twelve-bus three-region network from [13], [14], [15], [20] and [26].

We assume the same rotational inertia in all buses for a given time step t ($m_i(t) = m(t)$ for all i). This implies a similar fraction of renewable energy generation for all nodes, but this assumption can be easily extended. Each mode of the hybrid system is given by one value of inertia. For the study case we predefined possible inertia values for the system: $m_q \in \{0.2, 0.5, 1, 1.5, 2, 2.5, 3, 3.5, 5, 9\}$. The average of this set of possible inertia values is 2.8 seconds, which is equivalent to having 28 percent of thermal generation (10 s of inertia) and 72 percent of RES with zero inertia.

To generate the training set from (5) in II-B, each scenario s starts with 2 seconds of inertia, and from there– based

on a uniform distribution draw– the inertia (hybrid mode) of the system at time $t+1$ will remain the same, increase, or decrease. We assume that power electronics converters and batteries exist at every node as control agents to provide/absorb power. The time interval T_s we use is 0.01 seconds and the time horizon T is 400, equivalent to 4 seconds. For each scenario s, the initial states are drawn randomly from a normal distribution with zero mean and 1.3Hz of variance to represent different perturbations in the system. We simulate $S = 400$ scenarios.

To learn the controllers, we optimize (6) for each node using 100 possible values for the regularization parameter λ and a 10-fold cross-validation. This allows us to obtain 100 different controllers for each node. These controllers show decreasing number of features as λ increases, ranging from all 22 ($2n$) states down to zero. In order to analyze results we choose to study the performance, stability and feature selection of a subset of controllers. We group controllers by the number of features used, i.e. number of nonzero elements in β_i. Specifically, we choose a control design where all nodes use at most the following number of features: 4, 5, 6, 10, 14, 17, and all 22 states. To all the learned controllers we add virtual inertia as we describe in II-D. For the rest of the manuscript, each time we mention the learned controllers they also include virtual inertia.

B. Performance

In this section we explore the performance of the proposed learned controllers under different inertia modes for the hybrid system. Fig. 2 shows the box plot of the mean squared error (MSE) from training those controllers using cross-validation. As expected, the usage of more features allows to obtain a controller with reduced MSE in the training exercise. Nevertheless, the MSE does not significantly decrease beyond using 10 features. This sheds light on the possibility to substantially reduce the usage of features without losing significant performance. To show this we explore two performance metrics. One metric is the total absolute value of the control input and the other metric is the total absolute value of frequency deviation:

$$\langle u \rangle = \int_0^T \sum_{i=1}^{n} |u_i(t)| dt, \qquad \langle \omega \rangle = \int_0^T \sum_{i=1}^{n} |\omega_i(t)| dt$$

Table II shows the performance of the learned controllers with different numbers of features. We simulate the controllers on systems, different than the training set, with fixed low inertia ($m = 0.2$s) and fixed high inertia ($m = 9$s). In all simulations we consider an initial condition of -0.15Hz of frequency deviation at each node. Results in Table II show similar performance for the controllers with 10 or more features. The controllers with 6 and 5 features still perform well to steer the frequency deviation to zero, but they require more energy usage to achieve this. Fig. 3 depicts the frequency deviation evolution using the learned controllers for a system with inertia $m = 0.2$s. In the next section III-C we explore stability of the closed loop system with the proposed controllers, since, as observed in Table II, the learned controller with only 4 features is not stable.

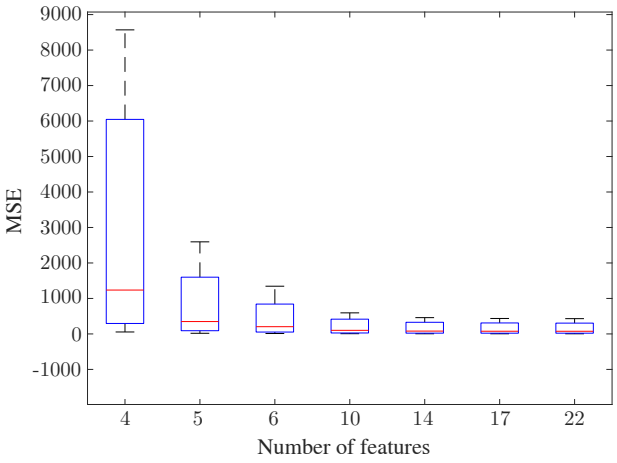

Fig. 2. Mean Squared Error (MSE) from training and cross-validating controllers with different numbers of features.

TABLE II
PERFORMANCE METRICS FOR LEARNED CONTROLLER UNDER DIFFERENT INERTIA SYSTEMS.

	$\langle u \rangle = \int_0^T \sum_{i=1}^n \lvert u_i(t) \rvert dt$		$\langle \omega \rangle = \int_0^T \sum_{i=1}^n \lvert \omega_i(t) \rvert dt$	
Number of features	$m = 0.2$s	$m = 9$ s	$m = 0.2$s	$m = 9$s
22	47.75	227.67	10.51	16.9
17	48.77	222.13	10.50	16.39
14	49.88	215.45	10.49	15.79
10	51.15	213.57	10.48	15.32
6	61.50	246.90	10.50	15.24
5	463.46	951.28	16.94	22.78
4	unstable	unstable	unstable	unstable

C. Stability analysis

We study stability in continuous time for the selected controllers. To do this, we calculate the eigenvalues of the closed loop system, derived from (5). We obtain

$$\dot{x} = (I - \hat{B}_{q(t)} \tilde{K}_V)^{-1} (\hat{A}_{q(t)} + \hat{B}_{q(t)} K_{\mathrm{L}}) x = A_{\mathrm{CL}(q(t))} x \qquad (9)$$

Our dynamical system is a hybrid system, thus we calculate eigenvalues for all possible inertia modes q. We find that all controllers in all inertia modes are stable except for the controller with 4 features. The controller with 4 features is unstable for all inertia modes. The case of 9 seconds of inertia is the closest case to being stable for the controller with four features. Fig. 4 shows all eigenvalues for the seven controllers in the 9 seconds inertia mode. We can observe how all controllers show eigenvalues with negative real parts, except the controller with 4 features which shows in black triangles four eigenvalues close to zero but positive and one eigenvalue equal to 0.93.

Fig. 5 plots the maximum among the real parts of the eigenvalues for each controller under different inertia modes. We choose the maximum real part of the eigenvalues as a metric of stability. In Fig. 5, as we also observe in Fig. 4, the controller with 4 features is unstable. The 9 seconds of

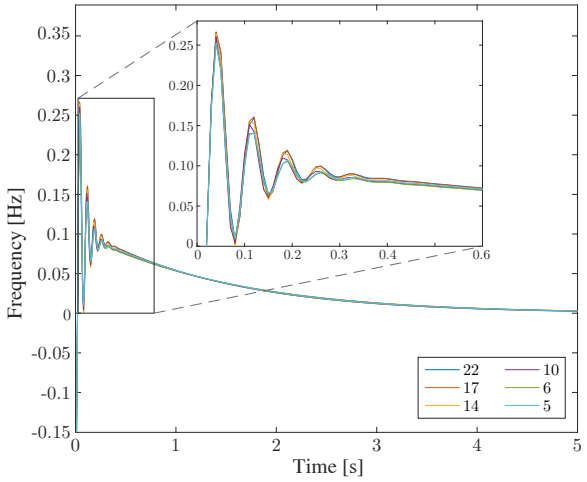

Fig. 3. Frequency deviation evolution using learned controllers with an initial deviation of -0.15Hz and a system's inertia of 0.2 seconds.

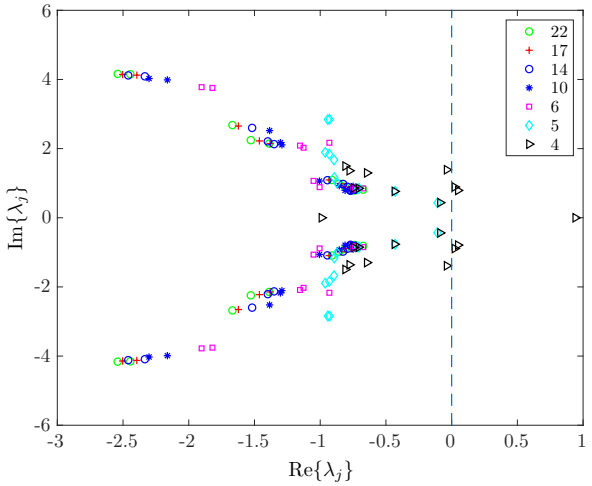

Fig. 4. Eigenvalues of all controllers j for the closed loop system with inertia of 9 seconds.

inertia mode is the closest it gets to attaining a non positive real part. As the system's inertia decreases, the maximum eigenvalue for this controller increases, potentially enhancing faster frequency deviations (more abrupt instability due to a faster exponential growth from the maximum positive real part). The observation where an increase of inertia results in a smaller maximum real part for the controller with 4 features cannot be observed for the other controllers. For these, their maximum eigenvalue real part occurs when the system shows it highest inertia ($m = 9$s). It is also relevant to notice that allowing the controller to have 6 or more features does not seem to impact the system's stability because the maximum real parts are similar.

D. Stability as a Switched-Affine hybrid system

In this section we study the stability of the hybrid system under *unconstrained switching* between modes. In other words, we are interested in studying the stability of the system if we allow any *adversarial* switching strategy (and

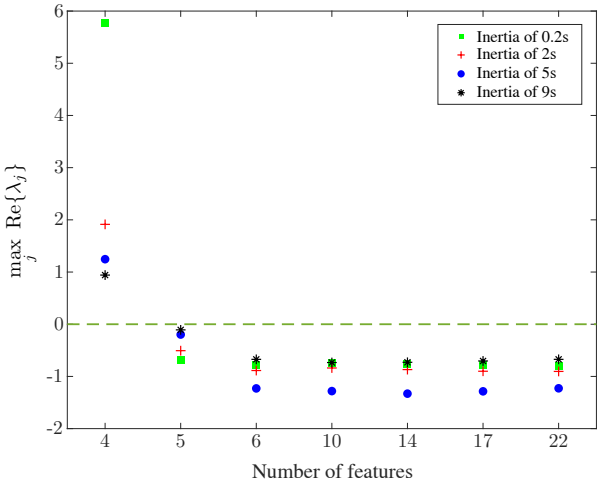

Fig. 5. Maximum eigenvalue real part for all controllers j under 0.2s (green square), 2s (red cross), 5s (blue dot) and 9s of inertia (black asterisk).

possibly not realistic) for inertia modes. For example, it would be possible to switch from $m = 9$s to $m = 0.2$s at any moment. It is a well known result that for a Switched-Affine hybrid system, even if all modes are stable independently, a switching sequence could potentially be found to make the hybrid system unstable [27].

A strategy to study stability of a hybrid system is to find a common Lyapunov function that ensures global asymptotic stability (in the sense of Lyapunov) over the set of all switching signals (Th. 1, p. 564 in [28]). The stability of a Switched-Affine hybrid system can be assessed by using a Lyapunov function of the form $V(x) = x^\top Px$, and by posing the following convex SDP problem:

$$\begin{aligned} \max_{P\in\mathbb{S}^{2n}, r\in\mathbb{R}, t\in\mathbb{R}} \quad & r+t \\ \text{s.t.} \quad & P \succeq rI_{2n\times 2n} \\ & A_{\text{CL}(q)}^\top P + PA_{\text{CL}(q)} \preceq -tI_{2n\times 2n},\ \forall q \in \{1,\dots,10\} \\ & \text{Trace}(P) = 1 \end{aligned}$$

where $\mathbb{S}^{2n}$ denotes the vector space of symmetric matrices of size $2n \times 2n$. If the optimal solution yields $r > 0$ and $t > 0$, then $P \succ 0$ and $\dot{V}(x) < 0$. This implies global asymptotically stability of the system. We solve the previous problem using CVX for all the proposed controllers. Results show that controllers with only 10 or more features achieve a global asymptotic stability for the hybrid system. This illustrates that despite the fact our sparse controllers with 6 or 5 features achieve stability on every inertia mode, under stressed cases of fast varying inertia the system may be unstable. Future work will explore realistic conditions for mode switching that would preserve stability of the hybrid system using our proposed controllers with 5 or 6 features. In particular, we will explore the required dwelling time τ_d that would guarantee stability (minimum time the system would have to maintain the same inertia).

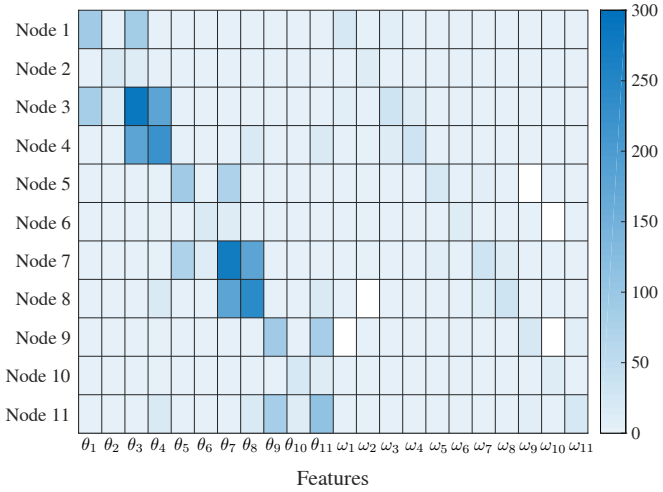

Fig. 6. Heat map of learned controller for $\lambda = 0$, meaning each node uses up to 22 features.

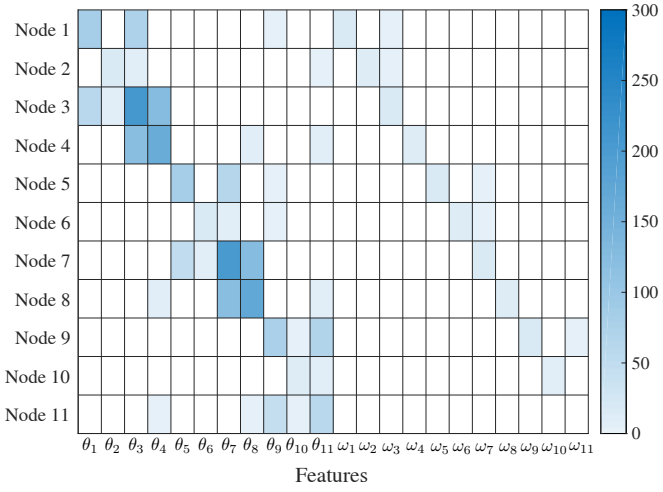

Fig. 7. Heat map of learned controller with λ-values tuned such that each node uses up to 5 features.

E. Optimal feature selection

In this section we explore which features are selected when we enhance sparsity in the learned controllers. Each controller (at each node) is allowed to use information of frequency and angles of any node in the system. This would require phasor measurement units (PMU) and instantaneous communication.

Fig. 6 depicts the heat map of the absolute value of the coefficients of the learned controller from the least-squares regression (i.e. $\lambda = 0$). The controllers prefer to use higher coefficients or gains in the angles than in frequency. It is important to notice that knowing the angles over time can be used to estimate changes of frequency as we show in equation (2). This explains the importance of angle states in feedback controllers. Nevertheless, a droop coefficient, related to their own local frequency, plays an important role in the stability of the closed loop system and is still considered critical in the regression. Feature selection in the learned controller with 4 features lacks coefficients on the frequencies (not pictured). This results in instability as we discuss in III-B and III-C.

In comparison, Fig. 7, depicts the heat map of the absolute value of the coefficients of the learned controller from the Lasso regression, with at most 5 features per node. In this case we can observe that a node's own angle and frequency tends to be critical to ensure stability of the system (except for node 11). However, information from other nodes is also required. In particular, voltage angles of connected nodes have an important role. For example, node 1 has an important coefficient in θ_3, that is the node connected to node 1 via a transformer. Similarly, node 3 uses information from θ_1, θ_2 and θ_4, which are connected via lines or transformers to that node (see Fig. 1). This shows the importance of the network connectivity to understand which features have crucial roles in the stability of the system. For future work, we are interested to study how topology and size of different networks can affect the selection of features.

F. Learning controllers from training sets with fixed inertia

To illustrate the importance of creating training sets from time-varying dynamics, we generate a separate training set using fixed inertia of $m = 0.2$s. We then train the controllers with this set and test the performance of the controllers with 22 features in a system with inertia $m = 0.2$s and $m = 9$s, and an initial frequency deviation. The controllers are able to stabilize frequency deviation around zero for both inertia regimes. However, when $m = 9$s they do not perform as well as the controllers learned from the time-varying inertia coefficients that we show in III-B.

We generate another separate training set using fixed inertia of $m = 9$s. We then train the controllers with this set and test the performance of the controllers with 22 features in a system with inertia $m = 0.2$s and $m = 9$. In this case, the controllers are able to stabilize frequency deviation around zero in the setting with $m = 9$s, but they are not able to steer it back to zero in the low inertia case ($m = 0.2$s).

From this exercise, we validate the importance of generating a training set with time-varying inertia. Training with these scenarios allows the learned controllers to be able to perform under different inertia regimes.

IV. CONCLUSIONS

In this paper we study how restricting communication between nodes affects the performance and stability of a time-invariant controller designed for time-varying power system dynamics due to RES. To do this, we generate a training set by solving an MPC formulation for different scenarios of frequency control. We design controllers with different numbers of features (states) via Lasso regressions. We add virtual inertia to these controllers to guarantee stability. For the 11-bus test system we study, we are able to show that it is possible to reduce the number of features in the controller (to 5 in our case study) without negatively impacting performance and stability for any fixed inertia of the system. We also show how increasing information avail-

ability beyond a threshold (10 features) does not enhance performance or stability metrics. We are able to show global asymptotic stability for the hybrid system using controllers with 10 features or more. Finally, by analyzing optimal feature selection for sparse controllers, we find a positive correlation between feature selection and connectivity of the nodes. For future work, we are interested to study how our results hold for different topologies and sizes of different networks.

Our work lies at the intersection of three control theory topics: time-invariant controllers for time-varying dynamics, information availability between control agents, and control design via learning. In this paper we are able to test performance and safety (stability) of a controller using this intersection of areas. However, safety is approached as a posterior analysis after the controller is designed. More interesting would be to design a controller with safety guarantees already built-in. This motivates our future work where we aim to develop a mathematical framework to design sparse time-invariant controllers via learning while at the same time guaranteeing stability of the closed loop system.

ACKNOWLEDGMENT

P.H.G. would like to thank the NSF Graduate Research Fellowships Program (GRFP). This work was also supported by NSF PIRE: Science of Design for Societal-Scale Cyber-Physical Systems (Award Number: UNIV59732), and by NSF awards 1539585 and 1646612.

REFERENCES

[1] J. Notenboom, P. Boot, R. Koelemeijer, and J. Ros, "Climate and Energy Roadmaps towards 2050 in north-western Europe: A concise overview of long-term climate and energy policies in Belgium, Denmark, France, Germany, the Netherlands and the United Kingdom," PBL Netherlands Environmental Assessment Agency, Netherlands, Tech. Rep., 2012.

[2] M. Wei, J. Nelson, M. Ting, C. Yang, D. Kammen, C. Jones, A. Mileva, J. Johnston, and R. Bharvirkar, "California's carbon challenge: Scenarios for achieving 80% emissions reductions in 2050," *Lawrence Berkeley National Laboratory, UC Berkeley, UC Davis, and Itron to the California Energy Commission*, 2012.

[3] I. Graabak and M. Korpas, "Variability characteristics of european wind and solar power resourcesa review," *Energies*, vol. 9, pp. 449–472, 2016.

[4] A. P. Kenneth and K. Folly, "Voltage rise issue with high penetration of grid connected pv," *IFAC Proceedings Volumes*, vol. 47, no. 3, pp. 4959 – 4966, 2014, 19th IFAC World Congress. [Online]. Available: http://www.sciencedirect.com/science/article/pii/S1474667016423839

[5] U.S. Department of Energy (DOE), "Maintaining Reliability in the Modern Power System," 2016.

[6] E. Ela, M. Milligan, and B. Kirby, "Operating reserves and variable generation," *Nat. Renew. Energy Lab., Golden, CO, USA*, Aug 2011.

[7] A. Ulbig, T. S. Borsche, and G. Andersson, "Impact of low rotational inertia on power system stability and operation," *IFAC Proceedings Volumes*, vol. 47, no. 3, pp. 7290–7297, 2014.

[8] H. Bevrani, T. Ise, and Y. Miura, "Virtual synchronous generators: A survey and new perspectives," *International Journal of Electrical Power & Energy Systems*, vol. 54, pp. 244–254, 2014.

[9] U. Tamrakar, D. Shrestha, M. Maharjan, B. P. Bhattarai, T. M. Hansen, and R. Tonkoski, "Virtual inertia: Current trends and future directions," *Applied Sciences*, vol. 7, no. 7, p. 654, 2017.

[10] Q.-C. Zhong and G. Weiss, "Synchronverters: Inverters that mimic synchronous generators," *IEEE Transactions on Industrial Electronics*, vol. 58, no. 4, pp. 1259–1267, 2011.

[11] E. Mallada, "idroop: A dynamic droop controller to decouple power grid's steady-state and dynamic performance," in *2016 IEEE 55th Conference on Decision and Control (CDC)*, Dec 2016, pp. 4957–4964.

[12] A. Ulbig, T. Rinke, S. Chatzivasileiadis, and G. Andersson, "Predictive control for real-time frequency regulation and rotational inertia provision in power systems," in *Decision and Control (CDC), 2013 IEEE 52nd Annual Conference on*. IEEE, 2013, pp. 2946–2953.

[13] T. S. Borsche, T. Liu, and D. J. Hill, "Effects of rotational inertia on power system damping and frequency transients," in *Decision and Control (CDC), 2015 54th IEEE Conference on*. IEEE, Dec 2015, pp. 5940–5946.

[14] B. K. Poolla, S. Bolognani, and F. Dörfler, "Optimal placement of virtual inertia in power grids," *IEEE Transactions on Automatic Control*, vol. 62, no. 12, pp. 6209–6220, 2017.

[15] P. Hidalgo-Gonzalez, D. S. Callaway, R. Dobbe, R. Henriquez-Auba, and C. J. Tomlin, "Frequency regulation in hybrid power dynamics with variable and low inertia due to renewable energy," in *2018 IEEE Conference on Decision and Control (CDC)*, Dec 2018, pp. 1592–1597.

[16] F. L. Lewis, D. Vrabie, and K. G. Vamvoudakis, "Reinforcement learning and feedback control: Using natural decision methods to design optimal adaptive controllers," *IEEE Control Systems Magazine*, vol. 32, no. 6, pp. 76–105, Dec 2012.

[17] K. L. Moore, *Iterative Learning Control: An Expository Overview*. Boston, MA: Birkhäuser Boston, 1999, pp. 151–214.

[18] O. Sondermeijer, R. Dobbe, D. Arnold, C. Tomlin, and T. Keviczky, "Regression-based inverter control for decentralized optimal power flow and voltage regulation," in *2016 IEEE Power Energy Society General Meeting (PESGM)*, 2016.

[19] F. Bellizio, S. Karagiannopoulos, P. Aristidou, and G. Hug, "Optimized local control for active distribution grids using machine learning techniques," in *2018 IEEE Power Energy Society General Meeting (PESGM)*, Aug 2018, pp. 1–5.

[20] P. Hidalgo-Gonzalez, R. Henriquez-Auba, D. S. Callaway, and C. J. Tomlin, "Frequency regulation using data-driven controllers in power grids with variable inertia due to renewable energy," in *IEEE PES General Meeting*. IEEE, August 2019.

[21] R. Dobbe, D. Fridovich-Keil, and C. J. Tomlin, "Fully decentralized policies for multi-agent systems: An information theoretic approach," in *NIPS*, 2017.

[22] R. Tibshirani, "Regression shrinkage and selection via the lasso," *Journal of the Royal Statistical Society. Series B (Methodological)*, vol. 58, no. 1, pp. 267–288, 1996. [Online]. Available: http://www.jstor.org/stable/2346178

[23] Electricity Reliability Council of Texas (ERCOT), "Future ancillary services in ERCOT," *ERCOT: Taylor, TX, USA*, 2013.

[24] M. Grant and S. Boyd, "CVX: Matlab software for disciplined convex programming, version 2.1," http://cvxr.com/cvx, Mar. 2014.

[25] F. Santosa and W. W. Symes, "Linear inversion of band-limited reflection seismograms," *SIAM Journal on Scientific and Statistical Computing*, vol. 4, no. 7, pp. 1307–1330, 1986.

[26] P. Kundur, "Power system stability and control," *McGraw-Hill*, 1994.

[27] M. S. Branicky, "Multiple lyapunov functions and other analysis tools for switched and hybrid systems," *IEEE Transactions on automatic control*, vol. 43, no. 4, pp. 475–482, 1998.

[28] R. Alur, K.-E. Arzen, J. Baillieul, and T. Henzinger, *Handbook of networked and embedded control systems*. Springer Science & Business Media, 2007.